Pis'ma v ZhETF

Magnetization of the $Mn_{1-x}Fe_xSi$ in high magnetic field up to 50 T: possible evidence of a field-induced Griffiths phase

S.V. Demishev [1,2], *A.N. Samarin* [1,3], *J. Huang* [4], *V.V. Glushkov* [1,3], *I.I. Lobanova* [1,3], *N.E. Sluchanko* [1,3], *N.M. Chubova* [5], *V.A. Dyadkin* [5,6], *S.V. Grigoriev* [5,7], *M.Yu. Kagan* [2,8], *J. Vanacken* [4], *and V.V. Moshchalkov* [4]

[1]*Prokhorov General Physics Institute of RAS, Vavilov street, 38, 119991 Moscow, Russia*

[2]*National Research University Higher School of Economics, Myasnitskaya street, 20, 101000 Moscow, Russia*

[3]*Moscow Institute of Physics and Technology, 9 Institutsky lane, Dolgoprudny 141700 Moscow region, Russia*

[4]*KU Leuven, Department of Physics and Astronomy, Celestijnenlaan 200D, B-3001 Leuven, Belgium*

[5]*Petersburg Nuclear Physics Institute, Gatchina, 188300 Saint-Petersburg, Russia*

[6]*Swiss-Norwegian Beamlines at the European Synchrotron Radiation Facility, 38000 Grenoble, France*

[7]*Saint-Petersburg State University, Ulyanovskaya 1, Saint-Petersburg, 198504, Russia*

[8]*Kapitza Institute for Physical Problems of RAS, Kosygina street, 2, Moscow, 119334, Russia*

Submitted 18 May 2016
Resubmitted today

Magnetic properties of single crystals of $Mn_{1-x}Fe_xSi$ solid solutions with $x < 0.2$ are investigated by pulsed field technique in magnetic fields up to 50 T. It is shown that magnetization of $Mn_{1-x}Fe_xSi$ in the paramagnetic phase follows power law $M(B) \sim B^{\alpha}$ with the exponents $\alpha \sim 0.33 - 0.5$, which starts above characteristic fields $B_c \sim 1.5-7$ T depending on the sample composition and lasts up to highest used magnetic field. Analysis of magnetization data including SQUID measurements in magnetic fields below 5 T suggests that this anomalous behavior may be likely attributed to the formation of a field-induced Griffiths phase in the presence of spin-polaron effects.

arXiv:1605.05519v2 [cond-mat.str-el] 6 Jun 2016

1. Substitutional solid solutions manganese monosilicide — iron monosilicide, $Mn_{1-x}Fe_xSi$ attract attention due to unique set of their physical properties, which include quantum critical phenomena [1,2], spiral magnetic order [3–5] and development of the magnetic phases with short-range magnetic order [1,2,6–10], similar to blue fog phases in liquid crystals [6–9] or to spin-liquid phases [10]. At the same time, the essential fundamental questions concerning the nature of magnetism in $Mn_{1-x}Fe_xSi$ system remain unsolved. It was taken for granted during decades that magnetic properties of MnSi, FeSi and MnSi based solids may be adequately described with the help of an itinerant model, which assumes a crucial role of spin fluctuations together with distributed spin density in the unit cell [11]. This point of view contradicts to recent electron spin resonance (ESR) experiments demonstrating localized character of magnetic moments in $Mn_{1-x}Fe_xSi$ [12,13] and to observation of the Yosida-type magnetic scattering [14] on localized magnetic moments, which dominates in magnetotransport properties [10,15]. Theoretical calculations in the framework of local density approximation (LDA) technique show that spin density in MnSi is localized on Mn ions, rather than being smeared [16]. It is worth noting that, in the fundamental work by Maleyev [17] as well as in the subsequent publications [3–5], the successful theoretical accounting of the magnetic properties of $Mn_{1-x}Fe_xSi$ is *de-facto* based on Heisenberg model of magnetism, i.e. implies presence of localized magnetic moments (LMM).

However, for resolving the paradigm of LMM-based magnetism in $Mn_{1-x}Fe_xSi$, it is necessary to explain the reduced value of saturated magnetization (less than Bohr magneton μ_B per Mn ion) when manganese LMM is about $\mu_{Mn} \sim 1.2\mu_B$ [16] and to suggest consistent explanation of ESR and magnetic scattering experiments [12,13,15] together with specific features of the field and temperature dependences of magnetization $M(B,T)$ [18]. For this purpose, a spin polaron phenomenological model was developed, where spin polaron represents a nanometer size quasi-bound state of itinerant electrons in the vicinity of manganese localized magnetic moments [12,15,18]. Opposite orientation of Mn

LMM and magnetic moments of band electrons results in reduction of the saturated magnetization and transitions of electrons between the quasi-bound and band states thus leading to spin fluctuations. This model construction is not confirmed by direct structural studies of the nanoscale so far, but spin polaron hypothesis has been successfully applied to the explanation of experimental data [12,13,15,18], which contradict to a widely accepted model of itinerant magnetism [11]. Moreover, as long as spin polaron represents an elementary ferrimagnet, the considered model opens an opportunity for natural interpretation of the recently discovered striking similarity between physical properties of metallic MnSi and ferrimagnetic dielectric Cu_2OSeO_3 with Heisenberg LMM [19], which cannot be either foreseen or explained in an itinerant model.

In order to make the right choice between the competing models of magnetism of $Mn_{1-x}Fe_xSi$, it is instructive to study magnetic properties in high magnetic fields. Indeed magnetic field may affect both spin fluctuations and spins alignment in spin polaron, so that analysis of the $M(B,T)$ data may shed more light on the origin of the magnetism in this system. At present there is a limited set of high field magnetization data for MnSi only, and field dependences $M(B, T = \text{const})$ are reported up to 50 T for the magnetically ordered spiral phase, and up to 30 T in the paramagnetic phase [20]. To the best of our knowledge, the magnetization of substitutional solid solutions $Mn_{1-x}Fe_xSi$ has never been examined in strong magnetic field. In the present work, we undertake the investigation of the magnetization in the paramagnetic phase of $Mn_{1-x}Fe_xSi$ with $x < 0.2$ in pulsed magnetic fields up to 50 T.

2. Single crystals of $Mn_{1-x}Fe_xSi$ with $x < 0.2$ investigated in the present work were identical to those studied in Ref. 2. The quality of the samples was controlled by X-ray and neutron diffraction. Samples composition was determined by electron probe micro-analysis (EPMA). The deviation from stoichiometric composition between metals (Fe, Mn) and silicon 1:1 did not exceed the value $\sim 0.5\%$ comparable with absolute error of our EPMA measurements. Field and temperature dependences of the magnetization in the magnetic field below 5 T were measured by using SQUID magnetometer (Quantum Design). Experiments in magnetic fields up to 50 T were conducted at KULeuven pulsed field facility [21] (Belgium). In all cases, the magnetic field was aligned along [110] direction. The temperatures, corresponding to the paramagnetic (PM) phase of $Mn_{1-x}Fe_xSi$ may be defined as $T > T_s(x)$, where $T_s(x)$ marks the transition into magnetic phase with short-range magnetic order [2,10]. The values of $T_s(x)$ were chosen in accordance with T-x magnetic phase diagram obtained in [2].

Pulsed field measurements of the magnetization field dependences were carried out with the help of the installation based on induction technique [22]. In our case, the difference with respect to Ref. 22 consisted in that the needle-like sample was located inside compensated pick-up coils. It is known that magnetization measurements of pure MnSi with pulsed magnetic field are affected by heating effects, which lead to complicated procedure of correct experimental differential of the $M(B)$ curve [20]. Heating of the sample may depend on thermodynamic contribution to free energy, which scales with the sample magnetization [20], and may be caused by Joule heating by induction currents in metallic $Mn_{1-x}Fe_xSi$ samples. For that reason, in order to reduce possible temperature variation, the samples of iron concentration $x = 0.054$, $x = 0.11$ and $x = 0.19$ were chosen for pulsed field experiments. In this concentration range magnetization of $Mn_{1-x}Fe_xSi$ is at least two times less than that of pure MnSi [2,15] and resistivity is about an order of magnitude higher.

For these samples the transition temperatures into the phase with short-range magnetic order are $T_s(x = 0.054) = 17.8$ K, $T_s(x = 0.11) = 8.9$ K and $T_s(x = 0.19) = 3.1$ K [2]. The sample with iron concentration $x = 0.054$ possesses Curie temperature $T_c = 12.6$ K, which is about 2.3 times less than in pure MnSi. At the same time, the transition into the phase with long-range magnetic order transition is strongly suppressed for $x \geq 0.11$ and does not exceed ~ 0.6 K [2,10].

As long as in induction pulsed field experiments both magnetization $M(t)$ and field $B(t)$ are functions of time t, change of the sample temperature will not be uniform during the pulse depending on the thermal exchange and thermal diffusion times. Careful comparative analysis of the $M(B)$ curves corresponding to pulses $B(t)$ with different magnitude allowed to conclude that the part of $M(t)$ pulse corresponding to increasing magnetic field was not affected by temperature variation in the studied samples. Therefore below we will consider only this part of pulsed field measurements, where the condition $T(t) = \text{const}$ is valid. Additional argument favoring the above assumption is the excellent reproduction of the $M(B)$ curves shape in pulsed field and steady field measurements performed at the same temperature. The latter observation also allowed using the magnetization curves obtained with the help of SQUID magnetometer for the absolute calibration of pulsed field data.

3. We first analyze $M(B)$ data in high magnetic fields. It is remarkable that up to the highest magnetic fields studied, field dependences of the magnetization in

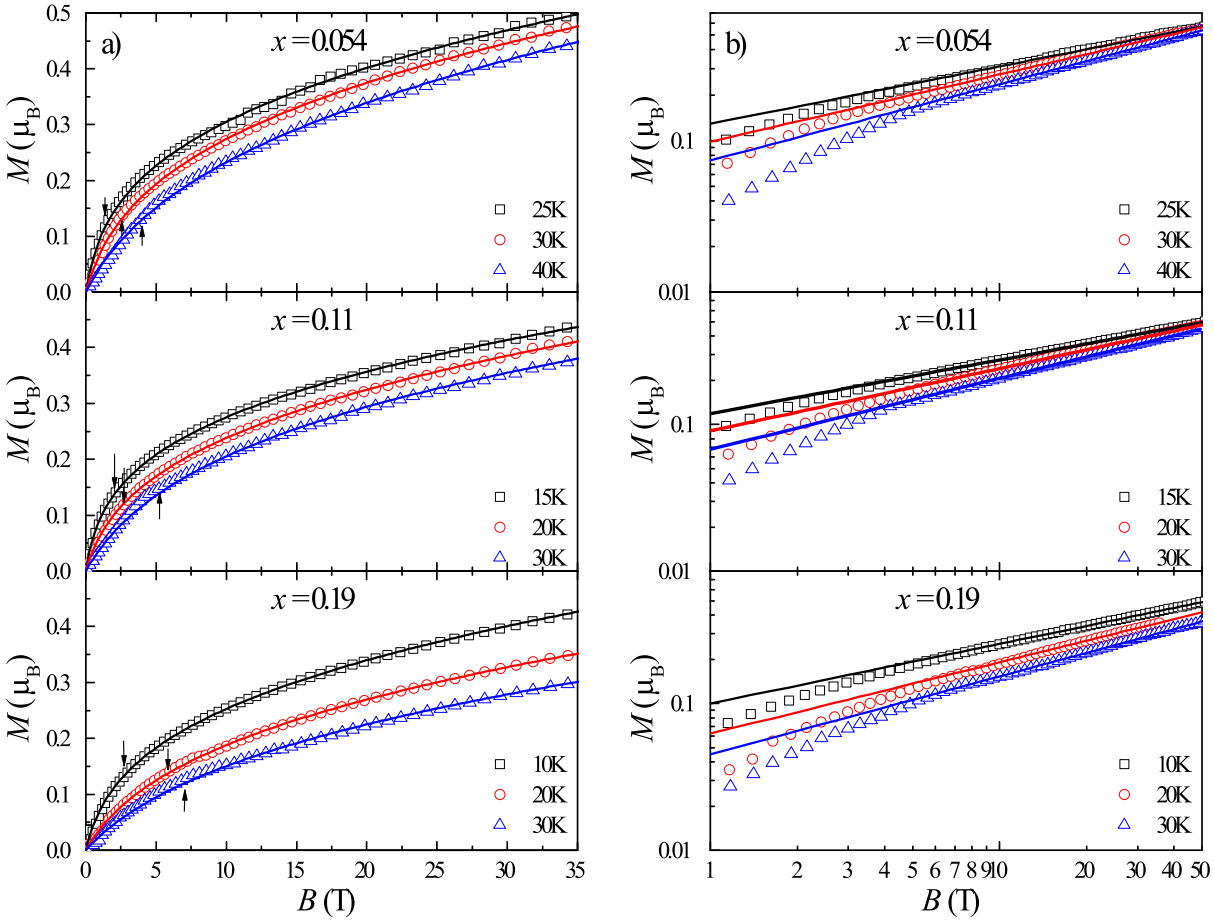

Fig. 1. Magnetization field dependences for $Mn_{1-x}Fe_xSi$. Points in the panels a, b — experiment, lines in the panel b — best fit by the power law (Equation 1), lines in the panel a — best fit with the help of interpolating formula (Equation 3). Arrows in the panel a denote crossover fields B_c.

the studied samples do not saturate (Fig. 1, panels a-b). Interesting that double logarithmic plot (Fig. 1,b) suggests high-field power behavior

$$M(B,T) = A(T) \cdot B^{\alpha(T)}, \qquad (1)$$

where both pre-factor A and exponent $\alpha < 1$ depend on temperature and concentration. This observation is very unusual, because since the pioneering work on MnSi [20] it is believed that magnetization in strong magnetic field increases linearly with constant slope, and therefore it is natural to expect similar behavior in $Mn_{1-x}Fe_xSi$ at least for the samples with low iron concentration.

In order to analyze high-field asymptotics of the magnetization field dependence in more detail, it is instructive to consider the function $F(B) = \partial M/\partial \ln B - M(B)$, which may be computed for each measured $M(B)$ curve. If Equation (1) is valid, the $F(B)$ is given by

$$F(B) = \frac{\partial M}{\partial \ln B} - M(B) = A(T) \cdot (\alpha(T) - 1) \cdot B^{\alpha(T)}, \qquad (2)$$

and hence in high magnetic field the $F(B)$ field dependence will reproduce the same power law except the case $\alpha = 1$, for which $F(B) \equiv 0$. In the case of a paramagnet with saturating magnetization $M(B \to \infty) = M_0$, the function $F(B)$ will also saturate at the value $F(B \to \infty) = -M_0$, because for $B \to \infty$ the derivative $\partial M/\partial \ln B$ turns to zero. Consequently the behavior of $F(B)$ allows discriminating between different cases, which may be expected for $Mn_{1-x}Fe_xSi$.

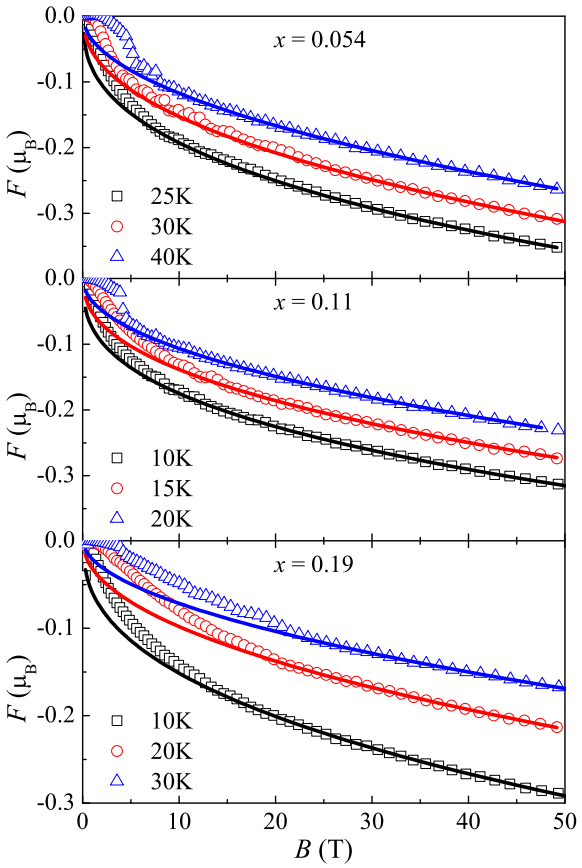

Fig. 2. Function $F(B)$. Points — calculation from experimental data in Fig. 1; lines — approximation by Equation (2). Parameters of the approximations are the same as in Fig. 1,b.

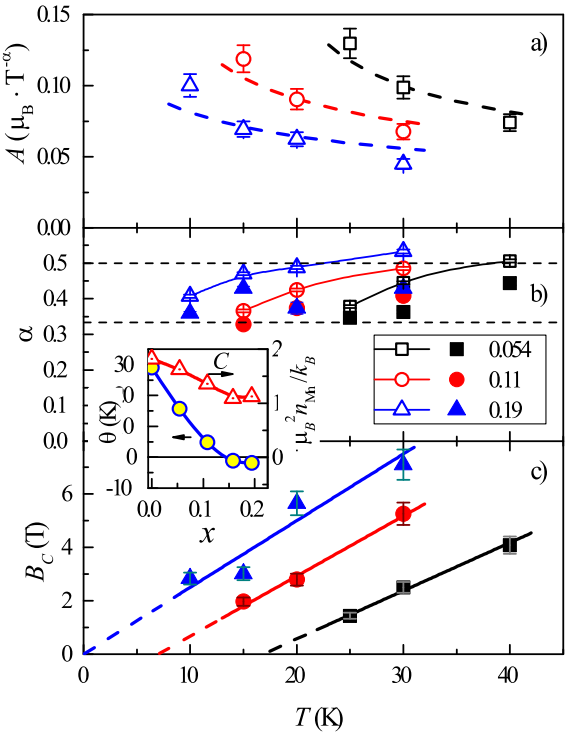

Fig. 3. Parameters in the model dependences: coefficient A in Equation 1 (panel a), the exponents α (panel b) and crossover fields B_c (panel c). Open symbols denote results obtained from fitting by Equation 1; solid symbols correspond to approximation with the help of interpolation Equation 3. Inset shows concentration dependences of Curie constant C and paramagnetic temperature θ obtained from the magnetic measurements in a low magnetic field.

Calculated functions $F(B)$ are presented in Fig. 2. It is visible, that the suggested in [20] form for high-field asymptotics $M(B) = M_0 + \chi^* \cdot B$, where χ^* denotes some effective susceptibility, does not meet experiment, as long as in this case $F(B)$ should saturate at some negative value. Instead of this, experimental data can be well fitted with the help of Equation (2) (solid lines in Fig. 2) with A and α as free parameters. The corresponding approximations by power law (1) with the same A and α are shown in Fig. 1,b (solid lines). The parameter $A(T)$ decreases with temperature and iron concentration (Fig. 3,b), whereas the exponent of the power law (1) demonstrates opposite behavior: $\alpha(T)$ increases with T and x and reaches value $\alpha(T) \sim 0.5$ at $T \sim 20 - 40$ K (open symbols in Fig. 3,b).

Now we will examine the region of a weak magnetic field. Straightforward analysis [23] shows that in the paramagnetic phase of $Mn_{1-x}Fe_xSi$ the Curie-Weiss asymptotics $M(B) = C \cdot B/(T-\theta)$ hold for temperatures which are higher by 1-3 K than $T_s(x)$ [10]. Hereafter C is Curie constant and parameter θ is denoted as the paramagnetic temperature. The parameters $C(x)$ and $\theta(x)$ decrease with x and the paramagnetic temperature changes sign at $x \sim 0.12 - 0.15$ (inset in Fig. 3). It is worth noting that the change of the sign of the Mn-Mn exchange energy J from ferromagnetic ($J > 0$) to antiferromagnetic ($J < 0$) was recently predicted for $Mn_{1-x}Fe_xSi$ with $x \sim 0.17$ [24]. The obtained dependence $\theta(x)$ reasonably concurs with this result.

In order to describe field-induced transformation of the Curie-Weiss linear dependence $M(B) \sim B$ into the power law $M(B) \sim B^\alpha$ the following interpolating formula may be used

$$M(B) = \frac{C}{T-\theta} \cdot \frac{B}{[B/B_c(T)+1]^{1-\alpha}}, \qquad (3)$$

where $B_c(T)$ denotes the crossover field. Equation (3) gives $M(B) = C \cdot B/(T-\theta)$ for $B \ll B_c(T)$ and corresponds to the power dependence (1) with $A(T) = C \cdot B_c^{1-\alpha}/(T-\theta)$ for $B \gg B_c(T)$. As long as parameters C and θ are known [23], the interpolating formula (3) provides two-parameter (B_c and α) approximation for a magnetization field dependence at fixed temperature. The results of fitting with the help of Equation (3) are presented in Fig. 1,a by solid lines. It is possible to conclude that this approach describes experimental data reasonably well. The obtained values of $B_c(T)$ are shown in Fig. 3,c and marked by arrows in Fig. 1,a. The crossover field increases with temperature almost linearly and extrapolation of the $B_c(T)$ dependence to the value $B_c = 0$ gives characteristic temperatures, which are very close to $\theta(x)$ (inset in Fig. 3). Therefore in the studied system $B_c(T)$ approximately follows the law $B_c \sim (T-\theta)$ with almost the same paramagnetic temperature as in Curie-Weiss asymptotics. In addition, the analysis of the experimental data by Equation (3) gives exponents $\alpha(T)$ which are somewhat different from those found from the power law approximation (see solid and open symbols in Fig. 3,b respectively). In the considered case, the average value is $\langle\alpha\rangle = 0.38 \pm 0.04$. Therefore it is possible to get an approximate expression for the coefficient A in the power law (1), $A(T) = C \cdot B_c^{1-\alpha}/(T-\theta) \approx A_0/(T-\theta)^{\langle\alpha\rangle}$, where A_0 is a numerical coefficient depending on C and dB_c/dT. Dashed line in Fig. 3,a are drawn in accordance with this estimate and it can be seen that deduced $A(T)$ function reasonably reproduces results of fitting by power dependence (1) without introducing any new free parameters. This consideration shows that the low magnetic field asymptotics and high magnetic field asymptotics of $M(B)$ are closely linked in $Mn_{1-x}Fe_xSi$, and Curie-Weiss behavior transforms into a power law when magnetic field increases.

4. The power asymptotics $M(B) \sim B^\alpha$, which are observed instead of saturated magnetization, are very unusual for several reasons. Firstly, existing theories predict the power law for magnetization when the system ground state is a Griffiths phase [25–30]. This behavior may be expected in magnetically disordered systems in the case $k_BT \ll \mu^*B$ with either ferromagnetic [29,30], or antiferromagnetic [28] interactions (here μ^* denotes the effective magnetic moment). The calculated values of the exponent α lie within limits $0.2 \le \alpha \le 0.6$ [28] or $1/3 \le \alpha \le 1/2$ [30] in agreement with the experimental data (Fig. 3,b). However, the aforementioned theoretical results were obtained for chain systems [28–30]. Moreover, in the early work [31] the field-induced crossover between $M(B) \sim B$ and $M(B) \sim B^\alpha$ was discovered in TCNQ based conducting spin chains, and was explained theoretically as a characteristic feature of just one-dimensional case without any disorder.

Apparently, $Mn_{1-x}Fe_xSi$ is a three-dimensional system, and results of Ref. 31 are not applicable to our case. At the same time, Griffiths phase scenario is more general [27,28], and in our opinion may be considered as a hypothesis to explain our results. Magnetic system in the Griffiths phase becomes separated into spin clusters due to spatial dispersion of exchange energies. The spin clusters with a higher (as compared to the average value) degree of correlation determine [26–30] the Griffiths phase magnetic properties. On a qualitative level, variations in temperature or magnetic field result in "scanning" over the randomly distributed spin clusters parameters [26,27] and this could lead to a departure from Curie-Weiss law for magnetic susceptibility $\chi(T)$ at low temperatures ($\chi(T)$ for $T \to 0$ diverges as a power of inversed temperature [26–30]) and to asymptotics $M(B) \sim B^\alpha$ [28–30]. However, in the studied case, no deviations from Curie-Weiss law in weak magnetic field are observed [23]. This means that if the concept of a Griffiths phase is applied to $Mn_{1-x}Fe_xSi$ samples studied in the present work, it is necessary to assume that Griffiths phase forms a high magnetic field $B > B_c$ and is missing in a weak magnetic field $B < B_c$.

Anyhow, the implementation of the Griffiths phase concept demands onset of magnetic inhomogeneity. This constitutes the second problem, as long as $Mn_{1-x}Fe_xSi$ is known as a system with strong spin fluctuations [11,13]. Spin density in itinerant magnetism model is distributed in the unit cell and this distribution is kept by spin fluctuations [11]. Therefore there is no way to obtain spatial magnetic inhomogeneity even in the case, when spin fluctuation rate is reduced in an external magnetic field. Therefore, the experimental results obtained in the present work do not favor itinerant description of magnetic properties of $Mn_{1-x}Fe_xSi$.

At the same time the application of the phenomenological spin-polaron model [18] is not straightforward. From one hand, as long as spin polarons are kind of magnetic inhomogeneities on the nanoscale, spin polaron paradigm looks promising for interpretation based on the Griffiths phase formation. According to [18], in the case when the concentration of electrons per Mn $n_e/n_{\rm Mn}$ satisfies inequality $n_e/n_{\rm Mn} < (\mu_{\rm Mn}/\mu_e)^2$ the magnetic subsystem of $Mn_{1-x}Fe_xSi$ will demonstrate magnetic phase separation into two types of magnetic states: spin polarons and bare Mn ions (here $\mu_{\rm Mn}$ and μ_e denotes magnetic moments of Mn LMM and band elec-

tron respectively). Repeating calculations of Ref. [18], it is possible to show that for any ratio of the numbers of spin-polaron states and bare Mn ions, Curie constant acquires the form $C = n_{\rm Mn}\mu_{\rm Mn}^2/k_B$, and therefore experimental data (inset in Fig. 3) correspond to the Mn localized magnetic moments $\mu_{\rm Mn} = (1.1 - 1.3)\mu_B$. This estimate correlate well with the LDA calculations, which give $\mu_{\rm Mn} = 1.2\mu_B$. Hall effect measurements give $n_e/n_{\rm Mn} = 0.9$ [24], so that condition for magnetic inhomogeneity is fulfilled for all $Mn_{1-x}Fe_xSi$ samples studied.

However, it is necessary to explain how possible magnetic inhomogeneity transforms in a strong magnetic field into disordered spin configuration specific to a Griffiths phase. This is hardly possible without elucidation of the microscopic nature of the proposed phenomenological spin-polaron model [18], which will be a subject of future investigations (both theoretical and experimental). Here we would like to make only several general remarks. First remark is connected with the correspondence between the spin-polaron state introduced for $Mn_{1-x}Fe_xSi$ [18] and the standard Nagaev-Mott-Kasuya-Krivoglaz [32–35] ferromagnetic (FM) polarons or ferrons, which appear in the antiferromagnetic (AFM) or PM matrices in the double-exchange model of De Gennes [36] or in the FM Kondo-lattice model (FM KLM). These models are relevant for manganites and other systems exhibiting colossal magnetoresistance phenomenon. It is possible to note many similarities between ferrons in the double exchange model and considered spin-polarons with respect to the percolative nature of the phase-transitions to FM state [37], the general expression for Curie-Weiss magnetic susceptibility in phase-separated state [38] and so on. At the same time, there is a striking difference in high magnetic field behavior, where ferrons are growing both at $T = 0$ and at finite temperatures [39], which leads to saturation of the magnetization instead of the power-law dependence in the studied case. Note that for ferrons description in the FM KLM we should have a FM sign ($J > 0$) of the exchange (Hunds) integral J between local spins and spins of conductivity electrons which are parallel for large J. As long as the sign of this exchange in $Mn_{1-x}Fe_xSi$ is not known exactly, and interaction of AFM nature cannot be excluded *a priori* (for example, in pure MnSi we should rather expect $J > 0$ in analogy with manganites, while in pure FeSi probably $J < 0$), then instead of FM KLM it will be necessary to consider an AFM KLM [40–42] with quite different physics. Namely, with large absolute values of J we may have the local singlets or generalized Kondo-singlets (totally screened or overscreened as in multi-channel KLM [41]). Note that in cuprates the local singlets on elementary CuO_4 plaquette are just famous Zhang-Rice singlets, which reduce the two-band Emery model to the one band t-J model [43]. When extending this analogy to the case of $Mn_{1-x}Fe_xSi$, we can possibly speak with some precautions about the totally screened (with respect to spin) or partially screened (ferrimagnetic) complexes consisting of 1 Mn ion and 1 or 2 conductivity electrons (or of even 2 neighbouring Mn ions and 2 or 3 conductivity electrons quasilocalized on these ions). It is worth noting that a complex structure of spin-polaron consisting of several Mn ions and electrons was introduced in [18]. Moreover, the application of the thermodynamic stability requirement [18] will result in allmost antiparallel configuration of local spins and spins of conductivity electrons in small magnetic fields. This picture, however, is an oversimplification again since it totally neglects the charge degrees of freedom. The more general situation corresponds to the periodic Anderson model [44] with strong hybridization of p-orbitals of Si and d-orbitals of transition element. Interesting, that according to Ref. 45 an intermediate mixed-valence state is expected for pure MnSi [45] and it is possible that the same situation holds in $Mn_{1-x}Fe_xSi$ for moderate Fe concentrations. This means that in correct microscopic model both spin and charge sectors should be taken into account on equal grounds. In particular, in charge sector an electron-polaron effect (connected with the interband Hubbard interaction) is very important [46–48]. In spin sector we should also consider the competition between the spin fluctuations and RKKY-interaction of Mn LMM expected for $Mn_{1-x}Fe_xSi$ [24], which may lead to a spin-glass phase (or a Griffiths phase) in agreement with generalized Mott-Doniach mechanism [49,50].

For substantial Fe concentrations it is possible to suppose that in high magnetic field $B > B_c(T)$ new magnetic phase, characterized by power law $M(B) \sim B^\alpha$ develops. In this case, the crossover field B_c may be linked with the spin fluctuations magnitude. For $B < B_c$ these fluctuations are strong enough and system is in paramagnetic phase, whereas for $B > B_c$ field-induced weakening of spin fluctuations gives way to a Griffiths-type magnetic phase. Moreover, it is natural to expect that crossover field may increase with temperature as long as the magnitude of spin fluctuations will increase with temperature in both itinerant [11] and spin-polaron models [13,18]. In addition, the increase of the spin fluctuations magnitude with iron concentration discovered in [13] should result in a corresponding enhancement of B_c. These qualitative speculations com-

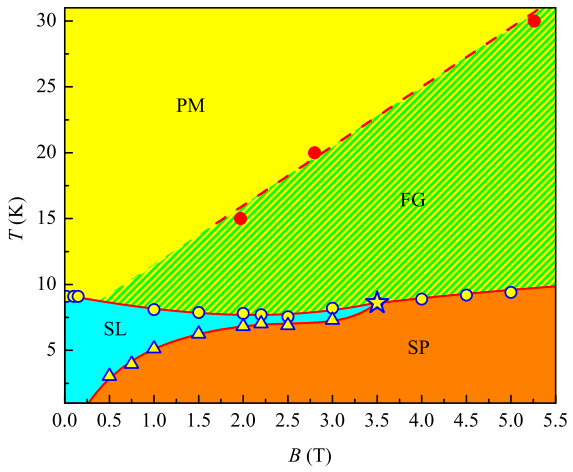

Fig. 4. Magnetic phase diagram for the sample with $x = 0.11$. Open symbols — data from Ref. 10, solid symbols — crossover field $B_c(T)$, which mark expected transition into field-induced Griffiths phase (FG). Different magnetic phases in accordance with Ref. 10 are paramagnetic phase (PM), spin-liquid phase (SL) and spin-polarized phase (SP).

pletely meet experiment, where $B_c(T, x)$ increases with both T and x (Fig. 3,c).

It is interesting to compare results of the present investigation with the phase diagram in a magnetic field recently obtained for the sample with $x = 0.11$ [10]. It was found that the magnetic phase diagram is formed by paramagnetic (PM), spin-liquid (SL) and spin-polarized (SP) phases (Fig. 4). This work adds new crossover line inside PM phase $B_c(T)$, which separate different regimes of spin fluctuations and marks onset of the field-induced Griffiths phase (FG) consisting of spin clusters. Successful application of the spin-polaron model for the explanation of the peculiarities in the paramagnetic phase strongly supports supposition that spin polarons may be considered as a "building blocks" for various magnetic phases in the case of $Mn_{1-x}Fe_xSi$ (Fig. 4). Within this concept we expect that the singular point discovered in [10] (star in Fig. 4) should be a triple point rather than a critical point as expected in spin-polaron scenario [10]. In strong magnetic field $B > 3.5$ T the increase in temperature at first leads to melting of the spin-polarized phase characterized by parallel spin alignment into special spin-cluster based phase (FG). Further increase of temperature will result in a crossover-type transition from FG with suppressed spin fluctuations to an effectively homogeneous PM phase with strong spin fluctuations (Fig. 4). More complicated behavior may be expected for intermediate fields $B \sim 1$ T, where variation of temperature may induce a sequence of phase transitions between the spin-polarized, spin-liquid, field-induced Griffiths and paramagnetic phases (Fig. 4). These phases may demonstrate different correlation lengths and regimes of spin fluctuations, so that physical picture in a magnetic field should go much further than often considered a simple fluctuation scenario for $B = 0$ [5,51]. For that reason we expect that additional studies of magnetic structure and magnetic fluctuations with the help of advanced neutron scattering technique could be rewarding and may shed more light on the nature of spin-polaron states and complicated magnetic phase diagram of $Mn_{1-x}Fe_xSi$ solid solutions.

5. In conclusion, we have shown that the magnetization of $Mn_{1-x}Fe_xSi$ in the paramagnetic phase follows power law $M(B) \sim B^{\alpha}$ with the exponents $\alpha \sim 0.33 - 0.5$, which starts above characteristic fields $B_c \sim 1.5 - 7$ T depending on the sample composition and lasts up to 50 T. In contrast to previous experimental and theoretical studies, the asymptotic $M(B) \sim B^{\alpha}$ behavior is observed in three-dimensional case rather than in one-dimensional spin chain system. This anomalous behavior may be attributed to the possible formation of a field-induced Griffiths phase presumably caused by spin-polaron effects.

Authors are grateful to D.I. Khomskii for helpful discussions. This work was supported by programmes of Russian Academy of Sciences "Electron spin resonance, spin-dependent electronic effects and spin technologies", "Electron correlations in strongly interacting systems". The work at KU Leuven was supported by the Methusalem Funding by the Flemish Government. M.Yu. K. thanks the Program of Basic Research of the National Research University Higher School of Economics for support.

1. A. Bauer, A. Neubauer, C. Franz, W. Mnzer, M. Garst, and C. Pfleiderer, Phys. Rev. B 82, 064404 (2010).
2. S.V. Demishev, I.I. Lobanova, V.V. Glushkov, T.V. Ischenko, N.E. Sluchanko, V.A. Dyadkin, N.M. Potapova and S.V. Grigoriev, JETP Lett. **98**, 829 (2013).
3. S.V. Grigoriev, V.A. Dyadkin, E.V. Moskvin, D. Lamago, Th. Wolf, H. Eckerlebe and S.V. Maleyev, Phys. Rev. B **79**, 144417 (2009).
4. S.V.Grigoriev, D.Chernyshov, V.A.Dyadkin, V.Dmitriev, E.V.Moskvin, D.Lamago, Th.Wolf, D.Menzel, J.Schoenes, S.V.Maleyev, and H.Eckerlebe, Phys. Rev. B **81**, 012408 (2010).
5. S.V.Grigoriev, E.V.Moskvin, V.A.Dyadkin, D.Lamago, T.Wolf, H.Eckerlebe, and S.V.Maleyev, Phys. Rev. B **83**, 224411 (2011).

6. A. Bauer and C. Pfleiderer, Phys. Rev. B **85**, 214418 (2012).
7. A.Hamann, D.Lamago, Th.Wolf, H.v.Lhneysen, and D.Reznik, Phys. Rev. Lett. **107**, 037207 (2011).
8. S. Tewari, D.Belitz, T.R.Kirkpatrick, Phys. Rev. Lett. **96**, 047207 (2006).
9. F. Kruger, U. Karahasanovic, A.G. Green, Phys. Rev. Lett. **108**, 067003 (2012).
10. S.V.Demishev, I.I.Lobanova, A.V.Bogach, V.V.Glushkov, V.Yu. Ivanov, T.V.Ischenko, N.A.Samarin, N.E.Sluchanko, S.Gabani, E.imr, K.Flachbart, N.M.Chubova, V.A.Dyadkin, S.V.Grigoriev, Pisma v ZhETF, **103**, 365 (2016).
11. T. Moriya, *Spin fluctuations in itinerant electron magnetism*, Berlin, Heidelberg, New York, Tokyo, Springer-Verlag, 1985.
12. S.V. Demishev, A.V. Semeno, A.V. Bogach, V.V. Glushkov, N.E. Sluchanko, N.A. Samarin, A.L. Chernobrovkin, JETP Lett. **93**, 213 (2011).
13. S.V.Demishev, A.N.Samarin, V.V.Glushkov, M.I.Gilmanov, I.I.Lobanova, N.A.Samarin, A.V.Semeno, N.E.Sluchanko, N.M.Chubova, V.A.Dyadkin, and S.V.Grigoriev, JETP Letters **100**, 28 (2014).
14. K. Yosida, Phys. Rev. **107**, 396 (1957).
15. S.V.Demishev, V.V.Glushkov, I.I.Lobanova, M.A.Anisimov, V.Yu.Ivanov, T.V.Ishchenko, M.S.Karasev, N.A.Samarin, N.E.Sluchanko, V.M.Zimin, and A.V.Semeno, Phys. Rev. B **85**, 045131 (2012).
16. M.Corti, F.Carbone, M.Filibian, Th.Jarlborg, A.A.Nugroho, P.Carretta, Phys. Rev. B **75**, 115111 (2007).
17. S.V.Maleyev, Phys. Rev. B **73**, 174402 (2006).
18. S.V.Demishev, T.V.Ishchenko, and A.N.Samarin, Low Temperature Physics **41**, 1243 (2015).
19. V.A. Sidorov, A.E. Petrova, P.S. Berdonosov, V.A. Dolgikh, and S.M. Stishov, Phys. Rev. B **89**, 100403(R) (2014).
20. T.Sakakibara, H.Mollymoto, and M.Date, J. Phys. Soc. Jpn. **51**, 2439 (1982).
21. J.Vanacken, T.Peng, J.A.A.J.Perenboom, F.Herlach, V.V.Moshchalkov, J. Low. Temp. Phys. **170**, 553 (2013).
22. A.S.Lagutin, J.Vanacken, N.Harrison, and F.Herlach, Review of Scientific Instruments **66**, 4267 (1995).
23. *See Supplemental Material at [URL to be inserted by publisher]*
24. V.V. Glushkov,I.I. Lobanova,V.Yu. Ivanov, V.V. Voronov, V.A. Dyadkin, N.M. Chubova, S.V.Grigoriev, and S.V. Demishev, Phys. Rev. Lett. **115**, 256601 (2015).
25. R.B.Griffiths, Phys. Rev. Lett. **23**, 17 (1969).
26. A.J.Bray, Phys. Rev. Lett. **59**, 586 (1987).
27. S.V.Demishev, Phys. Status Solidi B **247**, 676 (2010).
28. C.Dasgupta, S.Ma, Phys. Rev. B **22**, 1305 (1985).
29. D.S.Fisher, Phys. Rev. Lett. **69**, 534 (1992).
30. D.S.Fisher, Phys. Rev. B **51**, 6411 (1995).
31. L.N.Bulaevskii, A.V.Zvarykina, Yu.S. Karimov, R.B.Lyubovskii, I.F. Shchegolev, Soviet Physics JETP **35**, 384 (1972).
32. N.F. Mott, E.A. Davis, *Electronic processes in non-crystalline materials*, Clarendon Press, Oxford, 1971.
33. E.L. Nagaev, JETP Lett. **6**, 18 (1967), ibid. **27**, 122 (1968).
34. T. Kasuya, A. Yanase, T. Takeda, Solid State Commun. **8**, 1543, (1970).
35. M.A. Krivoglaz, Sov. Phys. Uspekhi **15**, 153 (1972), ibid. **16**, 856 (1974).
36. P.G. de Gennes, Phys. Rev. B **118**, 141 (1960).
37. M.Yu. Kagan, K.I. Kugel, Phys. Uspekhi **44**, 553 (2001).
38. M.Yu. Kagan, *Modern Trends in superconductivity and superfluidity, Chapters 15,16. Lecture Notes in Physics*, v.874, Springer, Dordrecht, 2013.
39. A.O. Sboychakov, A.L. Rakhmanov, K.I. Kugel, M.Yu. Kagan, I.V. Brodsky, JETP **95**, 753 (2002).
40. J. Kondo, Progr. Theor. Phys. **32**, 37 (1964).
41. A.M. Tsvelik, *Quantum field theory in condensed matter physics*, Cambridge University Press, 1998.
42. P. Fulde, *Electron correlations in molecules and solids*, Springer, Berlin, 1993.
43. F.C. Zhang, T.M. Rice, Phys. Rev. B **37**, 3759, (1988).
44. P.W. Anderson, J.Phys. C **3**, 2346 (1970).
45. F. Carbone, M.Zangrando, A. Brinkman, A. Nicolaou, F. Boudino, E. Magnano, A.A. Nugroho, F. Parmigiani, Th. Jarlborg, D. van der Marel, Phys. Rev. B **73**, 085114 (2006).
46. P. Nozieres, C.T. de Dominicis, Phys. Rev. **178**, 1097 (1969).
47. M.Yu. Kagan , N.V. Prokofev, JETP **63**, 1276 (1986), ibid **66**, 211 (1987).
48. M.Yu. Kagan, V.V. Valkov, JETP, v.140, p.179, 2011
49. N.F. Mott, *Metal-insulator transitions*, Taylor and Francis, 1974.
50. S. Doniach, Proc. Roy. Soc. **91**, 86 (1967).
51. M.Janoschek, M.Garst, A.Bauer, P.Krautscheid, R.Georgii, P.Bni, and C. Pfleiderer, Phys. Rev. B **87**, 134407 (2013).

Pis'ma v ZhETF

Magnetization of the $Mn_{1-x}Fe_xSi$ in high magnetic field up to 50 T: possible evidence of a field-induced Griffiths phase. Supplemental materials

S.V. Demishev [1,2], *A.N. Samarin* [1,3], *J. Huang* [4], *V.V. Glushkov* [1,3], *I.I. Lobanova* [1,3], *N.E. Sluchanko* [1,3], *N.M. Chubova* [5], *V.A. Dyadkin* [5,6], *S.V. Grigoriev* [5,7], *M.Yu. Kagan* [2,8], *J. Vanacken* [4], *and V.V. Moshchalkov* [4]

[1]*Prokhorov General Physics Institute of RAS, Vavilov street, 38, 119991 Moscow, Russia*

[2]*National Research University Higher School of Economics, Myasnitskaya street, 20, 101000 Moscow, Russia*

[3]*Moscow Institute of Physics and Technology, 9 Institutsky lane, Dolgoprudny 141700 Moscow region, Russia*

[4]*KU Leuven, Department of Physics and Astronomy, Celestijnenlaan 200D, B-3001 Leuven, Belgium*

[5]*Petersburg Nuclear Physics Institute, Gatchina, 188300 Saint-Petersburg, Russia*

[6]*Swiss-Norwegian Beamlines at the European Synchrotron Radiation Facility, 38000 Grenoble, France*

[7]*Saint-Petersburg State University, Ulyanovskaya 1, Saint-Petersburg, 198504, Russia*

[8]*Kapitza Institute for Physical Problems of RAS, Kosygina street, 2, Moscow, 119334, Russia*

Submitted 18 May 2016
Resubmitted today

arXiv:1605.05519v2 [cond-mat.str-el] 6 Jun 2016

Field dependences of magnetization at fixed temperatures $M(B, T = \text{const})$ were measured with the help of SQUID magnetometer (Quantum Design) up to $B = 5$ T for the $Mn_{1-x}Fe_xSi$ samples with iron concentration $x < 0.2$. Typical experimental results are shown in Fig. S1. Low field sections of $M(B, T = \text{const})$ curves were approximated by linear law $M(B,T) = \chi_0(T) \cdot B$ (lines in Fig. S1). The obtained $\chi_0(T)$ dependences for each particular sample were analyzed in coordinates $\chi_0^{-1} = f(T)$ (Fig. S2). The obtained $\chi_0^{-1} = f(T)$ dependences are linear and may be presented in the form $\chi_0^{-1} = (T - \theta)/C$ corresponding to Curie-Weiss law with Curie constant C and paramagnetic temperature θ. These parameters were found from linear fits of the data in Fig. S2 and shown at the inset in Fig. 3 of the main text.

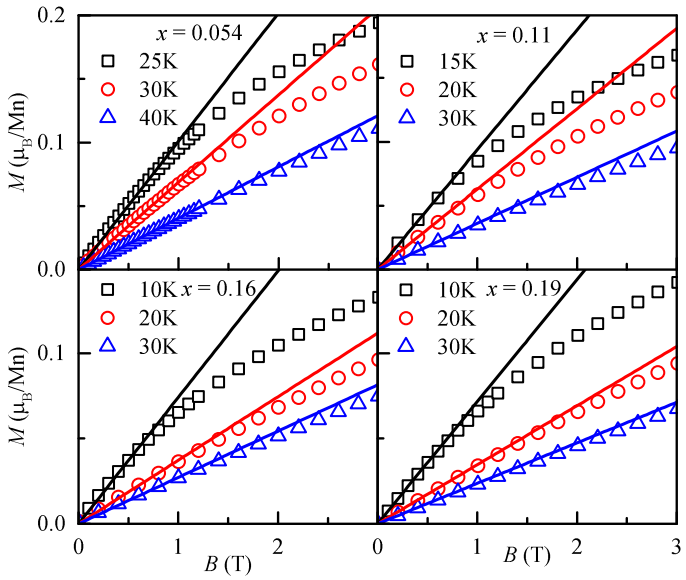

Fig. S1. Typical magnetization field dependences for different $Mn_{1-x}Fe_xSi$ samples in a weak magnetic field. Points — experiment, lines — approximation by linear law $M(B,T) = \chi_0(T) \cdot B$.

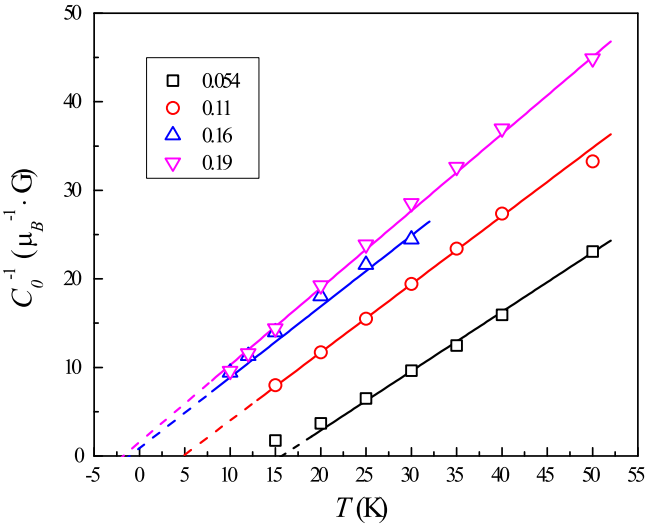

Fig. S2. Temperature dependences of the susceptibility $\chi_0(T)$ in coordinates $\chi_0^{-1} = f(T)$. Points — data obtained from analysis of the $M(B, T = \text{const})$ curves, lines — best fits with the help of equation $\chi_0^{-1} = (T - \theta)/C$.